16

Raman scattering and luminescence of $CoMF_6 \cdot 6H_2O$ (M = Si, Ge, Ti) activated by Mn^{4+} ions

© Yu.V. Pyastolova[1], A.S. Aleksandrovsky[1], N.M. Laptash[2], A.S. Krylov[1], A.A. Dubrovskiy[1]

[1] Kirensky Institute of Physics, Federal Research Center KSC SB, Russian Academy of Sciences, Krasnoyarsk, Akademgorodok, Russia,
[2] Institute of Chemistry, Far East Branch, Russian Academy of Sciences, Vladivostok, Russia,

E-mail: jul@iph.krasn.ru

Received November 20, 2024
Revised December 6, 2024
Accepted December 12, 2024

Mn^{4+}-doped red-emitting fluorides are a promising class of materials for improving the color rendering and luminous efficiency of white light-emitting diodes (WLEDs). Phosphors based on hydrated cobalt hexafluoridometallates $CoMF_6 \cdot 6H_2O$ (M = Si, Ge) activated with Mn^{4+} ions demonstrate red luminescence in the range of 600−650 nm upon excitation into the $^4A_2-^4T_2$ (450−480 nm) and $^4A_2-^4T_1$ (350−370 nm) bands. The luminescence spectra are formed by electron-phonon components at the $^2E-^4A_2$ transition involving vibrations of the MnF_6^{2-} octahedron. The quantum yield of $CoSiF_6 \cdot 6H_2O$: Mn^{4+} is maximized at 357 nm excitation and is equal to 5% at 5.5% manganese concentration. When the crystal lattice of $CoTiF_6 \cdot 6H_2O$ is formed, the depth of the potential minimum for the Mn^{4+} ion is smaller than in the case of $CoSiF_6 \cdot 6H_2O$ and $CoGeF_6 \cdot 6H_2O$, which leads to random fluctuations of the crystal field in the ensemble of positions occupied by this ion.

Keywords: red phosphor, fluorides, Mn^{4+}, Raman scattering, luminescence.

DOI: 10.61011/PSS.2024.12.60220.335

1. Introduction

Study of luminescent properties of various luminophore materials is of academic interest, but has practical value, too. Recently white light diodes (WLEDs) are widely used, being a new generation of solid-state sources of illumination due to their superb properties, such as high light output, energy-saving properties, long-term service life and absence of toxic mercury [1]. Most phosphors consist of microcrystalline matrix doped with an activator Various host-materials use lanthanide ions as luminescence activators in bivalent or trivalent charge state, however, in most crystalline luminophores and laser materials „non-rare earth“ tetravalent manganese ions (Mn^{4+}) are used successfully as optical activators [1–4]. Mn^{4+} ions most often activate oxides and fluorides and are the most studied ions of transition metals for light diode luminophores. Luminophores doped with Mn^{4+}, raised great interest due to simple availability of raw manganese rocks and low production costs. It is known that Mn^{4+} ions produce efficient red luminescence in the spectral range from 600 to 750 nm. New Mn^{4+}-activated luminophores of red glow based on fluoride and oxifluoride compounds correspond to the objective of efficiency and light quality of the future „warm“ devices of WLEDs. Within the wide family of inorganic fluorides with the common formula $ABF_6 \cdot 6H_2O$ (A — bivalent, B — tetravalent metal), luminophores are produced and described for a complex with zinc. Unique properties of hexahydrate phosphorus $ZnTiF_6 \cdot 6H_2O$:Mn^{4+}, emitting red light, are described [5,6]. For the first time the luminescent properties of $ZnSiF_6 \cdot 6H_2O$ and $ZnGeF_6 \cdot 6H_2O$, doped with various concentrations of Mn(IV), were described in [7], and their discussion continued in the papers by Hoshino & Adachi with recognition of these compounds to be interesting both from the scientific and technological points of view [8,9]. These authors also synthesized hexahydrate luminophore $ZnSnF_6 \cdot 6H_2O$:Mn^{4+}, emitting red light, and studied its unique structural and optical properties [10]. We attempted to synthesize a similar luminophore using hydrated compound of cobalt $CoSiF_6 \cdot 6H_2O$ and studied its optical properties [11]. In this paper we continue synthesis of luminophore based on hydrated fluoride metallates of cobalt (II) and present spectral studiesof crystals $CoGeF_6 \cdot 6H_2O$:$Mn^{4+}$and $CoTiF_6 \cdot 6H_2O$:Mn^{4+} compared to $CoSiF_6 \cdot 6H_2O$:Mn^{4+}.

According to the structural data, compounds $CoSiF_6 \cdot 6H_2O$ [12,13] and $CoTiF_6 \cdot 6H_2O$ [14] at room temperature are crystallized in the space group $R-3$, and $CoGeF_6 \cdot 6H_2O$ [15] in monoclinic one ($P2_1/c$). As the temperature decreases, the first two complexes undergo a phase transition to the monoclinic syngony ($P2_1/c$) at temperatures 246 K and 250 K accordingly, $CoGeF_6 \cdot 6H_2O$ undergoes phase transition to high-temperature phase at 338 K. In our studies we determine the spectral changes related to phase transitions at lower temperatures.

2. Experimental part

To synthesize the specimens of red luminophores $CoMF_6 \cdot 6H_2O$:Mn^{4+}(M = Si, Ge, Ti), source single crystals

Figure 1. Photographs of crystals and activated $CoMF_6 \cdot 6H_2O$:Mn^{4+} powder.

$CoMF_6 \cdot 6H_2O$ were used, which were produced from aqueous fluoride solutions. Chemically pure SiO_2 or GeO_2 were dissolved in HF (40 mass.%) with subsequent addition of stoichiometric quantity of $CoF_2 \cdot 4H_2O$ or $CoCO_3$. As a result of slow evaporation on air at room temperature, pink-brown crystals $CoSiF_6 \cdot 6H_2O$ and $CoGeF_6 \cdot 6H_2O$ were produced. Synthesis of $CoTiF_6 \cdot 6H_2O$ is described by us in [16], instead of TiO_2 we used the solution of oxidized titanium trichloride containing 47 mg/ml of titanium.

The Mn^{4+}-activator was K_2MnF_6 powder. 4 g of finely ground $KMnO_4$ and 60 g KHF_2 were dissolved in 200 ml HF (40 wt.%) and left in a tightly closed polyethylene container for the night in a refrigerator. H_2O_2 was added to the cold solution while stirring quickly in drops, until the solution color changed from purpose to red-brown, which indicated formation of Mn^{4+}. Golden-yellow sediment K_2MnF_6 was filtered, washed several times with acetone and dried at 70°C for 2 h. K_2MnF_6 (0.5 g) was dissolved in 10 ml HF (40%), heated on a water bath, then 5.5 g $CoMF_6 \cdot 6H_2O$, dissolved in 10 ml H_2O was added, and the solution was slightly evaporated to the first appearance of the crystalline film. The sediment produced after cooling was filtered, washed with alcohol and dried on air. According to the atomic absorption data, the product contained 5.5 at.% Mn in case of $CoSiF_6 \cdot 6H_2O$, 2.3 at% in $CoGeF_6 \cdot 6H_2O$ and 1.6 at% in $CoTiF_6 \cdot 6H_2O$. The data of X-ray powder diffraction of activated and pure crystals were identical and corresponds to PDF-2 data for $CoSiF_6 \cdot 6H_2O$ (№ 14–690), $CoGeF_6 \cdot 6H_2O$ (№ 078–2238) and $CoTiF_6 \cdot 6H_2O$ (№ 025–0257, in accordance with the publication [17]). The photos of the crystal and activated powder specimens are given in Figure 1. The powders of all activated Mn^{4+} crystals are identical in appearance.

Luminescence and photoluminescence excitation (PLE) spectra of the produced compounds were achieved in geometry 90° on spectrometer Shimadzu RF5301.

Raman scattering (RS) spectra were obtained using triple spectrometer Jobin Yvon T64000, equipped with a system of charge-coupled device (CCD) detection cooled with liquid nitrogen, in the mode of subtractive dispersion using backscattering geometry. Spectral resolution of Raman scattering spectra using lattices of 1800 strokes/mm and slots of 100 mcm made around 2 cm^{-1} (the system of micro-Raman scattering was built on the basis of microscope Olympus BX41 with lens $50 \times f = 1.2$ mm with numerical aperture NA = 0.75 provides for a focus spot with diameter of 4 μm on the specimen). The source of exciting light on the specimen was single-mode irradiation with wavelength $\lambda = 532$ nm from continuous laser Excelsior with diode pumping (Spectra-Physics) and power of 3 mW.

3. Experimental results and discussion

$CoSiF_6 \cdot 6H_2O$, $CoGeF_6 \cdot 6H_2O$, $CoTiF_6 \cdot 6H_2O$ crystals were studied by Raman scattering method; being activated with manganese ($CoMF_6 \cdot 6H_2O$:Mn^{4+}), they show luminescent properties.

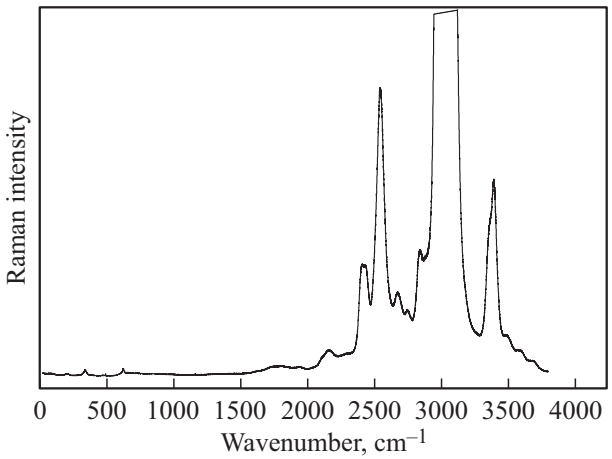

Figure 2. Panoramic spectrum of $CoGeF_6 \cdot 6H_2O$:Mn^{4+} compound emission in Raman scattering scale with pumping at 532 nm. The region below 1000 cm^{-1} contains Raman scattering lines, and in the region above 1000 cm^{-1} the luminescence contribution prevails.

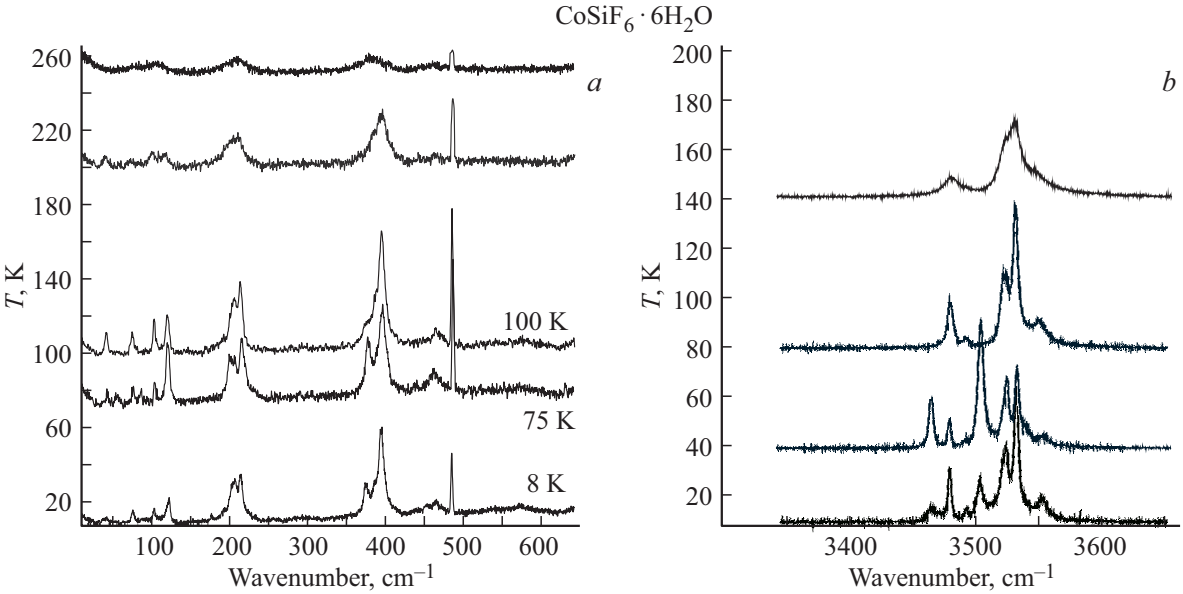

Figure 3. Raman scattering spectra $CoSiF_6 \cdot 6H_2O$ in the oscillation region of octahedron $[SiF_6]^{2-}$ and complex $[Co(H_2O)_6]^{2+}$ at different temperatures.

The Raman scattering method was used to obtain the spectrum of doped specimen $CoGeF_6 \cdot 6H_2O{:}Mn^{4+}$ (Figure 2).

One can see that the spectrum shows several intense lines in the region $2000-3500\,cm^{-1}$, the origin of which is due to luminescence of ion Mn^{4+}, which prevents the study of dynamics of the structural changes related to octahedrons $[MF_6]^{2-}$ and $[Co(H_2O)_6]^{2+}$. Therefore, it is feasible to obtain spectra from compounds, which do not contain ions Mn^{4+}. Crystal activation with manganese ions, as one should expect, does not change the dynamics of the lattice in the first approximation, where ions are involved, being the main for this crystal, including dynamics of the lattice at low temperatures.

Figure 3 presents Raman scattering spectra of $CoSiF_6 \cdot 6H_2O$ in the oscillation region of octahedron $[SiF_6]^{2-}$ and complex $[Co(H_2O)_6]^{2+}$ at different temperatures.

Previously we already published the study results of this compound [11]. It was found that the structural changes were related to ordering of octahedrons $[SiF_6]^{2-}$ and $[Co(H_2O)_6]^{2+}$, mediated with hydrogen bonds O-H $\cdots$ F (Figure 3). Contrary to $FeTiF_6 \cdot 6H_2O$, $FeTiF_6 \cdot 6D_2O$ previously studied by us, where octahedrons $[Fe(H_2O)_6]^{2+}$ and $[TiF_6]^{2-}$ are ordered independently as temperature decreases, in the studied crystal the ordering of octahedrons $[Co(H_2O)_6]^{2+}$ and $[SiF_6]^{2-}$ is interrelated.

Raman scattering spectra of single crystal $CoTiF_6 \cdot 6H_2O$ were obtained in the wide range of temperatures $8-300\,K$ and frequency range $11-4000\,cm^{-1}$.

RS spectra at $T = 220\,K$ show two rather wide bands corresponding to oscillations $[TiF_6]^{2-}$ (Figure 4). The mode ν_1 ($605\,cm^{-1}$) corresponds to symmetry A_{1g}, and the mode ν_5 ($300\,cm^{-1}$) — to F_{2g}. When temperature decreases, in the low-frequency region $80-250\,cm^{-1}$ weak lines appear. The spectral contour corresponding to the triple degenerate mode $\delta(TiF_6)$, undergoes changes (Figure 4). One can see well on the RS intensity map that at 40 K the frequencies of modes ν_1 and ν_5 steeply increase in average by $5\,cm^{-1}$.

The mode on $3500\,cm^{-1}$, corresponding to valence oscillation H_2O, breaks into doublet below 100 K (Figure 5), indicating rearrangement of hydrogen bods O-H $\cdots$ F. Formation of harder hydrogen bonds O-H $\cdots$ F caused steep change in the oscillation frequencies of the fluoride octahedron.

Temperature experiments in the vacuumized chamber at above 250 K led to the changes in the spectrum related to specimen degradation. After removal of the specimen from the chamber, small crystals of different colors were formed on the crystal surface [18]. One could see three colors in the incidence point of the laser beam: dark-purple Ti^{3+}, pale pink — Co^{2+}, and violet, most probably, Co^{3+}. Apparently, when exposed to laser beam, $CoTiF_6 \cdot 6H_2O$ is dissolved (melts) in its own crystallization water. Since the process is accompanied with charge transfer ($Co^{2+}+Ti^{4+} \rightarrow Co^{3+}+Ti^{3+}$), the melting process may be deemed incongruent (growth of crystals of different colors after irradiation removal). It is interesting that the red fluoride luminophore $ZnTiF_6 \cdot 6H_2O{:}Mn^{4+}$, demonstrating unique properties of luminescence, provided different spectra of photoluminescence under vacuum blowing or irradiation with visible-near UV-light, which may be explained by reactions of photooxidation and/or disproportionation of ions Mn^{4+} [6].

Based on the completed experiments, it should be concluded that phase transition below 100 K, the mechanism of

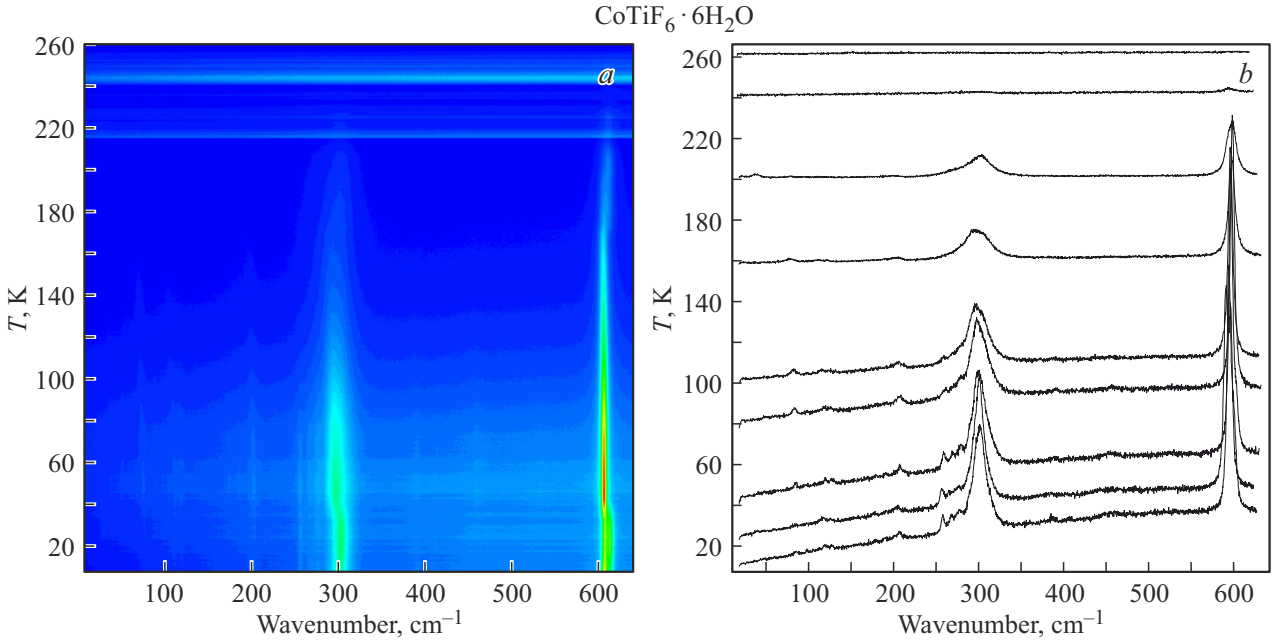

Figure 4. RS intensity map and RS spectra of $CoTiF_6 \cdot 6H_2O$ in the oscillation region of octahedron $[TiF_6]^{2-}$ at different temperatures.

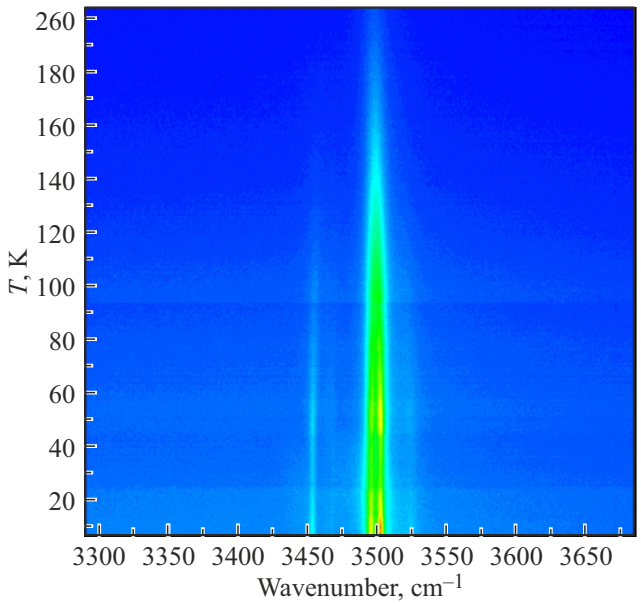

Figure 5. $CoTiF_6 \cdot 6H_2O$ RS intensity map in the region of valence oscillations H_2O of complex $[Co(H_2O)_6]^{2+}$ at different temperatures.

which is related to orientation rearrangement of hydrogen bonds, is being implemented in the studied compound.

RS spectra of $CoGeF_6 \cdot 6H_2O$ crystal were obtained as follows: the crystal was cooled down to temperature 8 K, and was heated up to 236 K (Figure 6) with slow temperature increase. In RS spectra in high-temperature phase the mode ν_1 (619 cm^{-1}) corresponds to symmetry A_{1g}, and the mode ν_5 (334 cm^{-1}) — to F_{2g}, related to oscillations of octahedron $[GeF_6]^{2-}$. When temperature decreases (Figure 6), in the low-frequency region 50–250 cm^{-1} weak lines appear.

In the low-temperature phase the spectral contour corresponding to triple degenerate mode $\delta(GeF_6)$ ν_5 (334 cm^{-1}), does not change (Figure 6), as well as the mode ν_1 (619 cm^{-1}). The mode corresponding to valence oscillation of water molecule, breaks into doublet below 100 K (Figure 7).

During temperature measurements, we observed a situation similar to $CoTiF_6 \cdot 6H_2O$, namely, formation of microcrystals of different color when exposed to laser irradiation and vacuum (Figure 8).

Since in $CoTiF_6 \cdot 6H_2O$ crystal this phenomenon was explained by change in valence state of Co and Ti ions, it should be assumed that in crystal $CoGeF_6 \cdot 6H_2O$ contrary to $CoTiF_6 \cdot 6H_2O$ this effect may only be related to the change in valence state of Co: $Co^{2+} \rightarrow Co^{3+}$. There is an alternative possibility, which consists in the fact that water evaporation causes radial structural rearrangement accompanied with strong increase of crystalline field on ion Co^{2+}. In $CoGeF_6 \cdot 6H_2O$ crystal the ground state of ion Co^{2+} has spin of 3/2, while in the strong crystalline field the ground state may be the state with spin of 1/2, for which absorption in the red area is specific, causing the violet color of microcrystal.

In this compound the structural phase transition is implemented below 100 K, provided for by the change in bonds O-H $\cdots$ F, while octahedron $[GeF_6]^{2-}$ remains ordered, which is indicated by the fact that the widths of modes corresponding to oscillations $[GeF_6]^{2-}$, practically do not depend on temperature, while the widths of modes corresponding to oscillations $[SiF_6]^{2-}$, decrease under cooling.

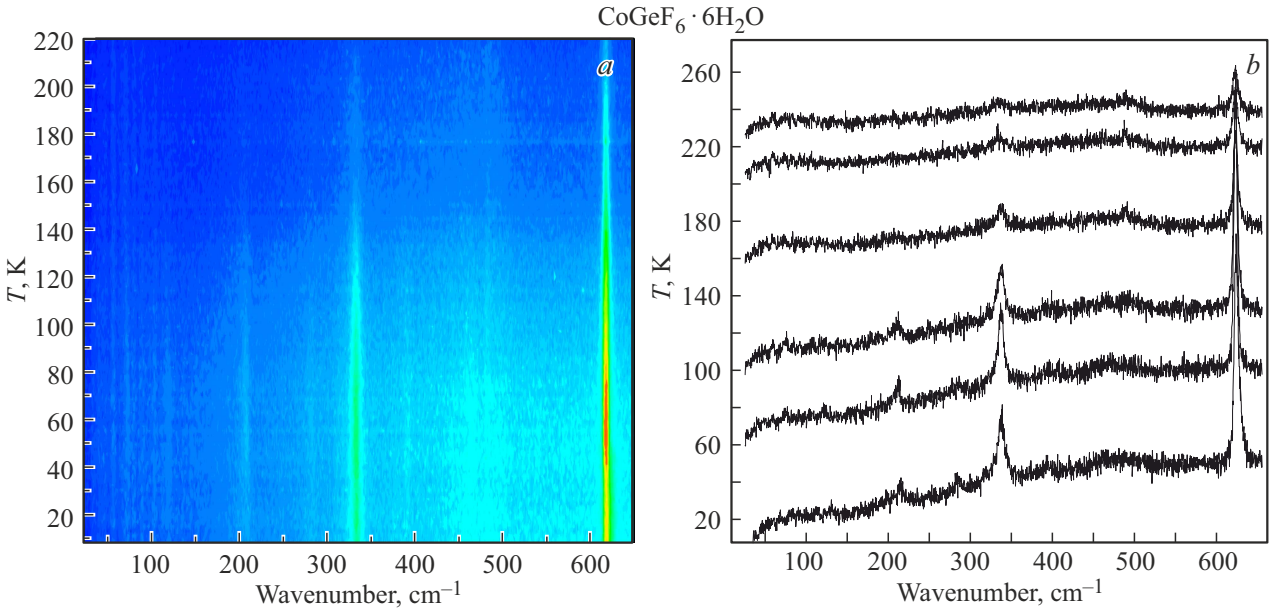

Figure 6. RS intensity map and RS spectra of $CoGeF_6 \cdot 6H_2O$ in the oscillation region of octahedron $[GeF_6]^{2-}$ at different temperatures.

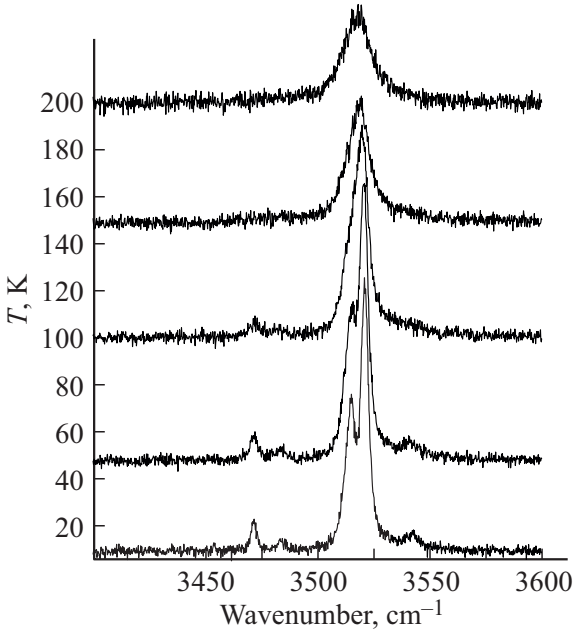

Figure 7. RS spectra of KP $CoGeF_6$ cot $6H_2O$ in valence oscillation region of H_2O octahedron $[Co(H_2O)_6]^{2+}$ at different temperatures.

Figure 9 shows luminescence spectra (in the right part of the curve) and luminescence excitation spectra (in the left part of the curve) for $CoGeF_6 \cdot 6H_2O{:}Mn^{4+}$, $CoSiF_6 \cdot 6H_2O{:}Mn^{4+}$ and $CoTiF_6 \cdot 6H_2O{:}Mn^{4+}$ crystals. Luminescence spectra of $CoGeF_6 \cdot 6H_2O{:}Mn^{4+}$ and $CoSiF_6 \cdot 6H_2O{:}Mn^{4+}$ crystals are practically identical, and the form of both spectra is explained by contribution of Stokes and anti-Stokes component of electron-phonon transition from state ^2E of ion Mn^{4+}. Octahedron $[MnF_6]^{2-}$ oscillation frequencies, determining the luminescence spectrum structure, are almost identical in both lattices. Luminescence excitation spectra in both crystals also have a similar structure and consist of two bands, corresponding to transitions of tetravalent manganese ion $^4A_{2g}-^4T_{2g}$ and $^4A_{2g}-^4T_{1g}$. The form and position of excitation bands in hydrated fluoride of cobalt-germanium and hydrated fluoride of cobalt-silicon are rather similar to each other. However, lattice $CoSiF_6 \cdot 6H_2O{:}Mn^{4+}$, where manganese ions substitute silicon ions, demonstrate a shift of excitation bands to a short-wave side compared to lattice $CoGeF_6 \cdot 6H_2O{:}Mn^{4+}$, accompanied by strong change in the ratio of bands towards the leveling of their

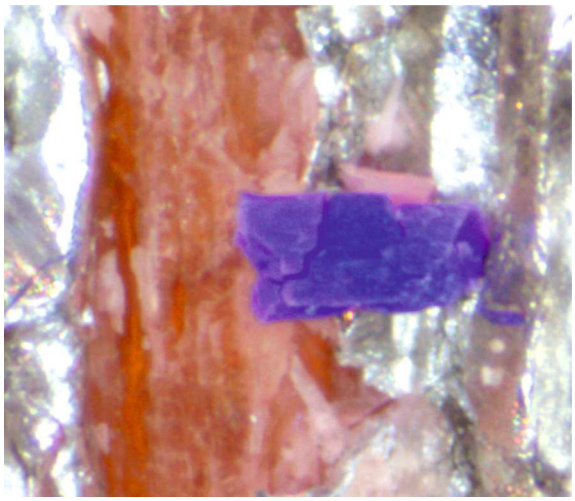

Figure 8. Photo of single crystal $CoGeF_6 \cdot 6H_2O$ after long-term exposure to laser irradiation in vacuum chamber.

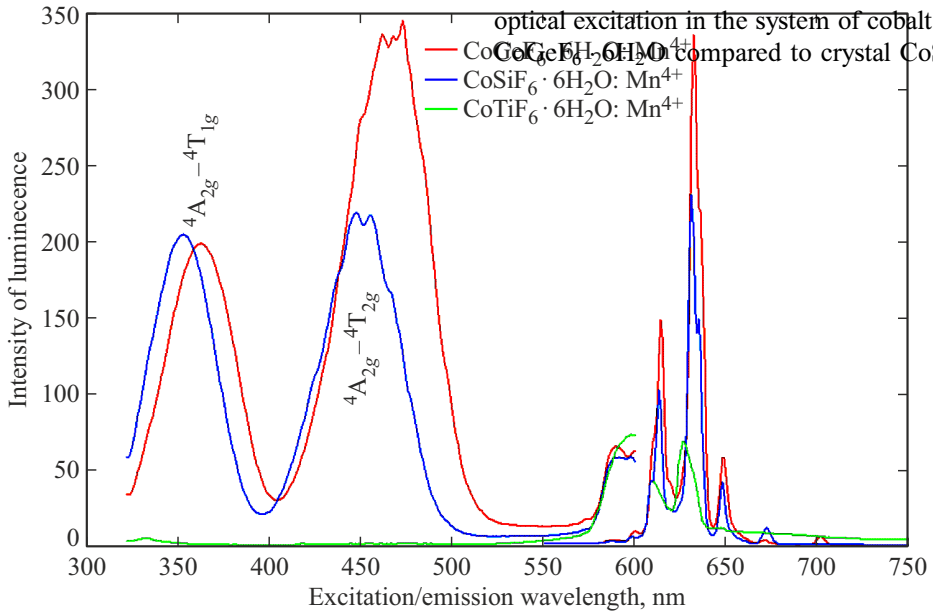

Figure 9. Luminescence spectra (right) and luminescence excitation spectra (left) of $CoMF_6 \cdot 6H_2O:Mn^{4+}$ crystals (M = Si, Ge, Ti), measured in 90-degree geometry.

amplitudes. Therefore, in crystal $CoSiF_6 \cdot 6H_2O:Mn^{4+}$ the power of crystalline field or the ratio of parameter of crystalline field to the Racah parameter is somewhat higher than in $CoGeF_6 \cdot 6H_2O:Mn^{4+}$. Crystal $CoTiF_6 \cdot 6H_2O:Mn^{4+}$ has luminescence in region 625 nm from manganese ion, however, its form is radically different from the form of luminescence spectrum of two other crystals, as well as its excitation spectrum, not containing bands specific for tetravalent manganese and related to transitions $^4A_{2g} - ^4T_{2g}$ and $^4A_{2g} - ^4T_{1g}$. The excitation band shifts to the red region of the spectrum ($\sim$ 600 nm), which may be related to transition $^4A_2 - ^2T_1$, feebly marked in case $K_2TiF_6:Mn^{4+}$ [19]. It should be noted that the position of the luminescent level ^2E, as well as level $^2T_1$ of ion Mn^{4+} according to the Tanabe-Sugano diagram, weakly depends on the crystalline field, whereas the position of levels ^4T, through which excitation is performed, depends strongly on the crystalline field. Therefore, presence of luminescence in the red region and absence of the marked absorption bands in the blue and ultraviolet regions (Figure 9) does not contradict the Tanabe-Sugano diagram for ion Mn^{4+}.

As we can see from the excitation spectra, the best agreement of the absorption band with the most beneficial light diode generation band is in case of $CoSiF_6 \cdot 6H_2O:Mn^{4+}$, but in case of $CoGeF_6 \cdot 6H_2O:Mn^{4+}$ the excitation in the blue region of the spectrum is quite efficient. The excitation spectrum of luminophores is in the red region of the spectrum, and quantum efficiency of luminescence in case of $CoSiF_6 \cdot 6H_2O:Mn^{4+}$ maximizes at 357 nm and makes 5% at rather high concentration of manganese 5.5%. In luminophore $CoGeF_6 \cdot 6H_2O:Mn^{4+}$ the quantum efficiency is 3%, which should be attributed to nonradiative relaxation of optical excitation in the system of cobalt ion levels in crystal $CoGeF_6 \cdot 6H_2O$ compared to crystal $CoSiF_6 \cdot 6H_2O$.

4. Conclusion

Synthesis of luminophores based on hydrated fluoride metallates of cobalt (II) and the study of their spectral properties have shown that the concentration quenching in luminophores $CoSiF_6 \cdot 6H_2O:Mn^{4+}$ and $CoGeF_6 \cdot 6H_2O:Mn^{4+}$ was rather moderate. The optimal concentration of activator in $CoSiF_6 \cdot 6H_2O:Mn^{4+}$ is 5.5 percent, and quantum efficiency at excitation of 357 nm — 5%.

In the row of the studied crystals $CoSiF_6 \cdot 6H_2O$, $CoTiF_6 \cdot 6H_2O$, $CoGeF_6 \cdot 6H_2O$ the transitions are implemented, which depend on the selection of M(IV). In $CoSiF_6 \cdot 6H_2O$ the structural transitions are accompanied by interrelated rearrangement of both anion and cation substructures. In $CoTiF_6 \cdot 6H_2O$ the rearrangement of hydrogen bonds results in the change in the anion substructure. In crystal $CoGeF_6 \cdot 6H_2O$ the anion substructure remains unchanged, and changes are related to rearrangement in the system of hydrogen bonds O-H $\cdots$ F.

Funding

The work was done with financial support from the Russian Science Foundation, the Government of Krasnoyarsk Krai and the Krasnoyarsk Krai Foundation of Science within the research project No. 23-22-10037.

Conflict of interest

The authors declare that they have no conflict of interest.

References

[1] G.B. Nair, H.C. Swart, S.J. Dhoble. Progr. Mater. Sci. **109**, 100622 (2020).
[2] S. Adachi. ECS J. Solid State Sci. Technol. **9**, 016001 (2020).
[3] S. Adachi. ECS J. Solid State Sci. Technol. **10**, 026002 (2021).
[4] S. Adachi. J. Lumin. **263**, 119993 (2023).
[5] J. Zhong, D. Chen, X. Wang, L. Chen, H. Yu, Z. Ji, W. Xiang. J. Alloys Compd. **662**, 232–239 (2016).
[6] R. Hoshino, S. Sakurai, T. Nakamura, S. Adachi. J. Lumin. **184**, 160–168 (2017).
[7] M. Kubus, D. Enseling, T. Justel, H.-J. Meyer. J. Lumin. **137**, 88 (2013).
[8] R. Hoshino, S. Adachi. J. Appl. Phys. **114**, 213502 (2013).
[9] R. Hoshino, S. Adachi. J. Lumin. **162**, 63 (2015).
[10] R. Hoshino, S. Adachi. Opt. Mater. **48**, 36 (2015).
[11] Yu.V. Gerasimova, A.S. Aleksandrovsky, N.M. Laptash, A.S. Krylov, M.A. Gerasimov, A.A. Dubrovskiy. Opt. Mater. **144**, 114343 (2023).
[12] H. Lynton, P-Y. Siew. Can. J. Chem. **51**, 227 (1973).
[13] S. Ray, A. Zalkin, D.H. Templeton. Acta Cryst. **29**, 2741 (1973).
[14] A.A. Udovenko, E.B. Merkulov, D.Kh. Shlyk, N.M. Laptash. ZhSKh, **65**, 11 (2024). (in Russian).
[15] B.F. Hoskins, A. Linden. Austr. J. Chem. **40**, 565 (1987).
[16] S.V. Melnikova, N.M. Laptash, E.I. Pogoreltsev. J. Fluorine Chem., **263**, 110048 (2022).
[17] R.L. Davidovich, T.A. Kaidalova, T.F. Levchishina. Zh. Strukt. Khim. **12**, 185 (1971).
[18] V.V. Korochentsev, N.M. Laptash, Solid State Sci. **148**, 107433 (2024).
[19] T. Senden, R.J.A. van Dijk-Moes, A. Meijerink. Light: Sci. Appl. **7**, 8 (2018).

Translated by M.Verenikina